Bulletin of Earthquake Engineering
https://doi.org/10.1007/s10518-024-01904-1

ORIGINAL ARTICLE

Seismic behaviour of Exterior RC beam-column joints repaired and strengthened using post-tensioned metal straps

Yasser Helal[1] · Reyes Garcia[2] · Thanongsak Imjai[3] · Pakjira Aosai[3] · Maurizio Guadagnini[4] · Kypros Pilakoutas[4]

Received: 20 October 2023 / Accepted: 22 March 2024

Abstract
Exterior beam-column joints are the most vulnerable part of substandard reinforced concrete (RC) buildings and are often the first to be damaged during earthquakes. This article presents an experimental and numerical investigation into the behaviour of exterior RC beam-column joints repaired and strengthened using Post-Tensioned Metal Straps (PTMS) for active confinement. The study focused on full-scale beam-column joints with an inadequate core zone detailing, thus emulating the deficiencies found in existing substandard RC buildings. Initially, four "bare" joints were subjected to cyclic tests to induce substantial damage within the core zone. Subsequently, the damaged core of the joints was repaired and recast with new concrete, and PTMS were applied to strengthen the joints, followed by another round of cyclic testing. The experimental findings were compared with predictions generated through established models from existing literature. The results revealed that ASCE/SEI 41–17 guidelines accurately predict the shear capacity of the bare joints. It is shown that recasting the core with new concrete significantly increased the joint's shear capacity by up to 42% compared their bare counterparts. The use of PTMS strengthening further enhanced the capacity by up to 25%. A "scissors model" was employed for numerical simulations of both bare and PTMS-strengthened joints using DRAIN-2DX, which proved effective at predicting their nonlinear load-displacement envelope response. This article contributes towards the development of new cost-effective post-earthquake strengthening techniques for beam-column joints, with the potential to reduce the vulnerability of substandard RC buildings in developing countries.

Keywords *Beam-column joints · Reinforced concrete · Seismic strengthening · Concrete repairs · Post-tensioned metal straps · Numerical modelling*

Extended author information available on the last page of the article

1 Introduction

Numerous reinforced concrete (RC) buildings have suffered extensive damage or complete collapse during recent major earthquakes (e.g. Indonesia 2018, Haiti 2021, Afghanistan 2022, Turkey-Syria 2023, Morocco 2023). Such devastating events resulted in significant financial and human losses. Many of the failures observed in these vulnerable RC buildings can be attributed to the inadequate detaling of beam-column joints. In particular, insufficient steel reinforcement in the core zone and inadequate shear capacity have been identified as significant factors contributing to these failures (Garcia et al. 2014a; Khan et al. 2018b; Sianko et al. 2020). Addressing these issues through local strengthening of substandard joints represents a practical solution to mitigate the vulnerability and potential losses from seismic events in developing countries.

Empirical vidence gathered from buildings damaged in past earthquakes underscores the high susceptibility of exterior joints to shear failures. This vulnerability is primarily attributed to the abrupt changes in geometry and to the limited confinement provided by adjacent elements. Consequently, various strengthening techniques have been proposed to increase the shear capacity of substandard exterior joints. One such method involves the application of stiffening steel plates (see Fig. 1a) that are securely affixed around joints to increase their shear capacity by up to 35% over unstrengthned control joints (Torabi et al. 2017). Diagonal haunches (Fig. 1b) were proven to increase the shear capacity of joints by 53-76% (Dang et al. 2017, Truong et al. 2017; Zabihi et al. 2018), and led to a more desirable beam hinging failure. Moreover, the cumulative energy dissipated by joints with diagonal haunches was up to 4.48 times that of control joints (Dang et al. 2017) due to a change from a joint

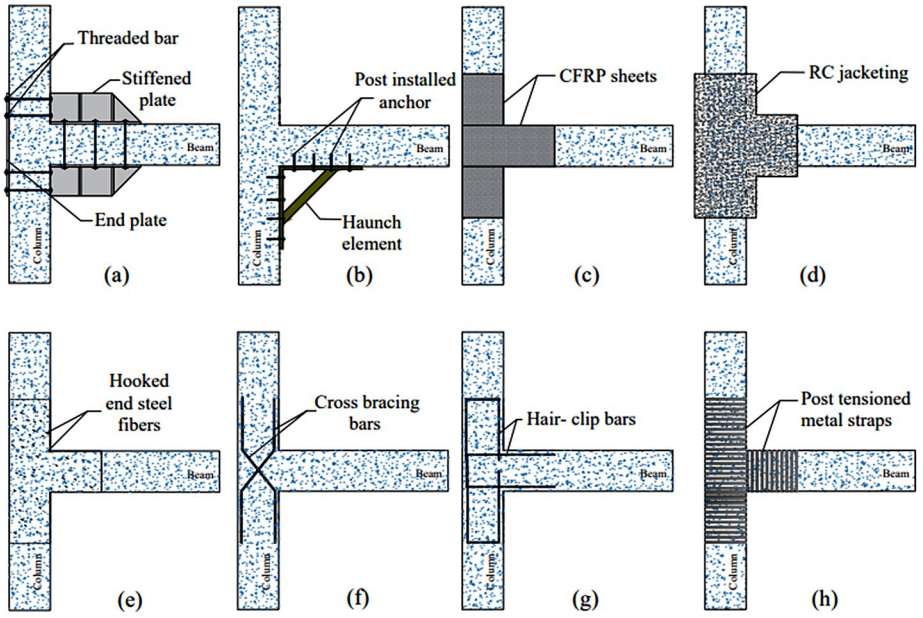

Fig. 1 Different strengthening techniques for exterior beam-column joints (**a**) stiffeneing steel plates, (**b**) single diagonal haunch, (**c**) FRP jackets, (**d**) RC jackets, (**e**) SFRC jackets, (**f**) cross bracing bars, (**g**) hair clip bars, and (**h**) Post-Tensioned Metal Straps

shear failure (J-type) to a mixed flexural-shear failure (JB-type failure) (Kanchanadevi and Ramanjaneyulu 2021).

Utilising externally bonded Fibre Reinforced Polymer (FRP) jackets (see Fig. 1c) has proven to be higly effective for enhancing the capacity (by about 64-148%) and ductility (by about 51-74%) of substandard exterior joints when compared to control specimens (Singh et al. 2014; Mostofinejad and Akhlaghi 2017; Wang et al. 2019; Mostofinejad and Hajrasouliha 2019; Obaidat et al. 2019). Nonetheless, the initial cost of FRP materials can present a barrier to their wide application, particularly in developing countries where material costs account for most of the strengthening budget.

In addition to FRP jacketing, alternative methods have demonstrated their effectiveness in enhancing the capacity, ductility, and energy dissipation of joints as rehabilitation methods. These methods include jacketing with RC (Fig. 1d), ultra-high-performance fibre reinforced concrete (UHPFRC), steel fibre-reinforced concrete (SFRC) (Fig. 1e), or steel fibre-reinforced geopolymer mortar (Sharma and Bansal 2019; Khan et al. 2018b; Ruano et al. 2014, Choudhury and Lascar 2021). These methods can increase the capacity of joints by up to 66%, ductility by up to 62% and and energy dissipation by up 113% over control joints. However, it should be noted that concrete or mortar jacketing can increase member size and mass the structure, potentially altering its dynamic properties (Bindhu et al. 2016, Kalogeropoulos et al. 2016).

Other techniques (Muthupriya et al. 2014; Bindhu and Jaya 2010) involve the use of diagonally-crossed bracing bars within the joint core (Fig. 1f), that can significantly increase the ductility of joints by up to 115%. Another technique by Rajagopal and Prabavathy (2015) involves the use of mechanical anchorages with hair clips (Fig. 1g) with a 90^{o} bent to enhance capacity (by up to 12%) and ductility (by up to 37%) over bare joints. It should be noted that whilst these techniques can effectively enhance the shear capacicty and ductility of joints, they predominantly provide “passive confinement” to concrete. To date only limited studies (e.g. Huang et al. 2023) have investigated the effectiveness of prestressing techniques in improving the behaviour of substandard beam-column joints. Such “active confinement” techniques hold potential for further enhancing the seismic performance of these critical structural elements, thus preventing potential collapses during strong earthquakes.

Research by Frangou et al. (1995) proposed a novel technique that uses Post Tensioned Metal Straps (PTMS) to strengthen concrete elements. In this technique, high-strength metal straps are wrapped around concrete components using a pneumatic tensioning tool, thus applying “active confinement” (Garcia et al. 2017; Imjai et al. 2020a, b). Moghaddam et al. (2010) demonstrated that PTMS confinement increased the strength of concrete cylinders by up to 25% over counterpart specimens with equivalent passive confinement. PTMS confinement was also effective at enhancing the strength and ductility of high-strength concrete (HSC) cylinders and columns tested in compression (Ma et al. 2015; Chin et al. 2018, Ma et al. 2018). PTMS have been effectively used to increase the capacity of shear-dominated RC beams by up to 63% (Setkit and Imjai 2019; Setkit et al. 2020, Abdullah 2023), as well as the bond strength of short spliced RC beams by up to 58% (Helal et al. 2016; Helal et al. 2016). Garcia et al. (2014a) used PTMS confinement to strengthen a substandard RC building subjected to shake-table tests. The PTMS strengthening significantly enhanced the seismic resistance of the building from a peak ground acceleration of PGA=0.15 g to a PGA=0.35 g. However, due to the global nature of shake table tests on whole structures,

the results did not provide sufficient insight into the behaviour of beam-column joints. Yang et al. (2019) investigated the post-fire shear behaviour of RC T-beams strengthened with prestressed steel straps. The results indicate that the post-fire shear capacity of strengthened T-beams was up to 138% higher compared to counterpart unstrengthened beams.

Although previous research has validated the effectiveness of the PTMS technique in enhancing the performance of various structural components, it is worth noting that no studies have explored the specific use of PTMS in improving the behavior of substandard RC beam-column joints. This represents an important research gap that warrants further investigation to assess the potential benefits and effectiveness of PTMS in addressing the specific challenges posed by these critical structural elements. This article addresses this critical research gap by investigating the seismic performance of exterior RC beam-column joints when strengthened with PTMS. In the initial stage, four substandard joints were intentionally subjected to reverse cyclic loading to produce significant damage in the core zone. Subsequently, the damaged core of the joints was repaired/recast with new concrete, and the joints were then strengthened with PTMS to repeat the cyclic tests. The study's findings are presented and discussed in terms of observed damage, load-drift behaviour and cummulative energy dissipation. The contextualize the results, the experimental findings are compared to predictions generated according to established models in the literature. Furthermore, the joints are modelled in DRAIN-2DX software adopting a "scissors model" to calculate their nonlinear envelope response. This research holds significant implications for the development of new post-earthquake strengthening techniques for beam-column joints. Ultimately, these advancements have the potential to substantially reduce the vulnerability of substandard RC buildings in developing countries, contributing to enhanced seismic resilience and safety.

2 Experimental programme

2.1 Geometry and reinforcement of joints

Four susbtandard RC beam-column joint specimens were designed to simulate part of a connection between two floors in a multi-storey moment-resisting frame, but without a slab. The column height was 2700 mm with cross-section dimensions of 260×260 mm (Fig. 2a). The beam length was 1650 mm from the face of the column to the free end, with a cross-section of 260×400 mm. The beam and column were longitudinally reinforced with bars of diameter ϕ16 mm, as shown in Fig. 2a. The longitudinal reinforcement of the column was spliced with a length of 400 mm (i.e. 25ϕ) just above the core zone. The beam was also reinforced longitudinally with ϕ16 mm bars. The cross-section dimensions and flexural/shear reinforcement of the beam and columns of the tested joints were similar to those of a deficient RC building subjected to shake table tests by the authors (Garcia et al. 2010). Such building was originally designed with old European earthquake-resistant provisions from the 60's and with no transverse shear reinforcement at the core zone of the joints, so as to ensure that a shear failure occurred at that location. The longitudinal reinforcement of the beam was anchored into the core with different lengths and bent lengths (types A, B or C), according to the detailing shown in Fig. 2b. These anchored lengths were insufficient

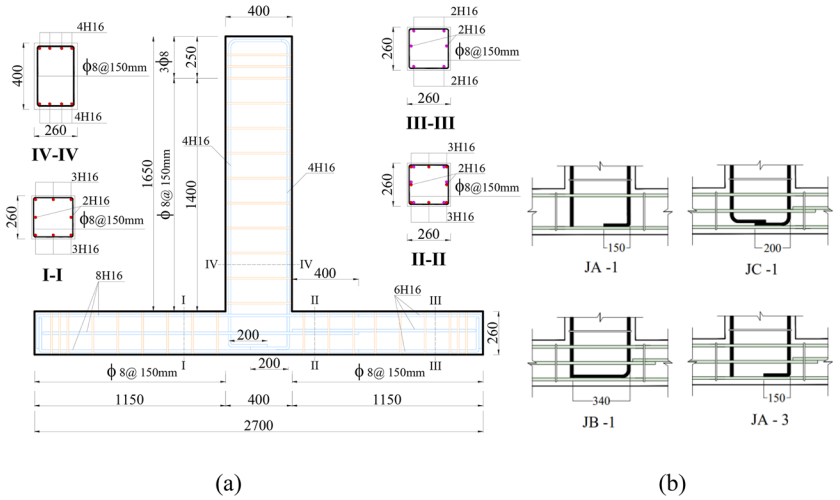

Fig. 2 Tested joints (**a**) geometry and reinforcement detailing, (**b**) detailing of longitudinal beam reinforcement into the core (units: mm)

to develop the full yield strength of the beam bars, simulating inadequately designed joints found in seismically damaged structures.

The transverse reinforcement of both beam and column consisted of fully closed stirrups of diameter ϕ8 mm at 150 mm centres (Fig. 2a). This transeverse reinforcement was sufficient to prevent shear failures in these elements. No transverse reinforcement was provided in the core zone of the joint in order to replicate typical substandard construction practices of buildings in developing countries. The lack of transverse shear reinforcement in the joint area was designed to ensure that a shear failure occurs in the core zone before the flexural capacity of the beam was attained. The theoretical beam flexural capacity was calculated to be 144 kNm, whereas the column flexural capacity was 72 kNm for a column axial load ratio of 11% (axial load of 250 kN, joint JA-3). The column-to-beam relative flexural strength ratio ($\Sigma M_{Rcol}/\Sigma M_{Rbeam}$) was 1.0, thus resulting in an inadequate strong beam-weak column strength hierarchy. The joints were identified with an ID in which the first letter "J" stands for "joint", the second letter stands for the type of longitudinal beam detailing in the core (A, B, or C), and a number indicates the number of the specimen. The "PTMS" abbreviation in the ID indicates that the joint was repaired (recast core) and subsequently strengthened using PTMS.

2.2 Material properties

The joints were cast using three batches of premixed concrete. The mean concrete compressive strength (f_{cm}) was determined from tests on three 150×300 mm concrete cylinders according to BS EN 12390-3 (BSI 2009a). The indirect tensile splitting strength (f_{ct}) was obtained from tests on three 100×200 mm cylinders according to BS EN 12390-6 (BSI 2009b). All cylinders were cast at the same time and cured together with the joints. Table 1 summarises the mean values (average of three cylinders) and standard deviations (SD in square brackets) of the compressive and split tensile strengths obtained from the tests. The

Table 1 Concrete properties of beam-column joints

Condition	ID	f_{cm} (MPa) [SD]	f_{ct} (MPa) [SD]
Bare	JA-1	22.5 [±0.59]	2.6 [±0.14]
	JA-3	31.4 [±0.75]	2.4 [±0.06]
	JB-1	28.6 [±1.05]	2.5 [±0.02]
	JC-1	28.6 [±0.95]	2.5 [±0.05]
Repaired and PTMS-strengthened	JA-1PTMS	85.0[a] [±0.20]	4.5 [±0.12]
	JA-3PTMS	39.3 [±0.83]	2.5 [±0.08]
	JB-1PTMS	56.2 [±0.57]	3.4 [±0.10]
	JC-1PTMS	57.0 [±1.00]	3.6 [±0.03]

[a] Steel Fibre Reinforced Concrete (SFRC) mix

table also includes the properties of the concrete used to repair/recast the damaged core zone of the joints after the initial tests.

Due to difficulties in finding low-strength steel bars as those typically available in developing countries, the reinforcing steel of the joints consisted of ribbed bars grade S500. Compared to low-strength steel bars, the use of deformed bars S500 was more critical because the joints could be subjected to higher force and bond demands. The yield and tensile strengths of the reinforcement were obtained from four bar coupons tested in direct tension. These values were found to be f_y=630 MPa and f_u=760 MPa for the 8 mm bar, and f_y=555 MPa and f_u=690 MPa for the 16 mm bar, respectively. The metal straps used to strengthen the joints had f_y=930 and f_u=1030 MPa, and a modulus of elasticity E=202 GPa.

2.3 Test setup and instrumentation

The joints were tested with the column placed horizontally, as shown in Fig. 3. Pin supports at the ends of the column simulated the points of contraflexure of the column. A hydraulic jack was used to apply axial load on the column. The axial load on the column of joints JA-1, JB-1 and JC-1 was 150 kN (i.e. axial load ratio of 7-9%), whereas JA-3 was loaded with a load of 250 kN (axial load ratio 11%). Cyclic load was applied on the beam through a two-hinged actuator. The loading protocol consisted of a series of displacement-control steps (see Fig. 4) applied as drift ratio (DR) percentages. Each DR had three push-pull cycles applied at a rate of 0.4 mm/min. The initial tests on the bare joints were halted when the maximum load recorded in the test dropped by approximately 50%.

Before the initial tests, the joints were white-washed to facilitate the observation and marking of cracks. Sixteen potentiometers were then mounted on the joint area, lap splice region and potential beam hinging zone. This facilitated capturing deformations due to crack opening at the beam-column interfaces, as well as deformations within the core. Figure 5 shows a typical bare joint with potentiometers. Ten Linear Variable Differential Transducers (LVDTs) measured deflections at the tip of the beam, supports, lateral displacements along the beam, and movement of the stiff frame used to test the joints.

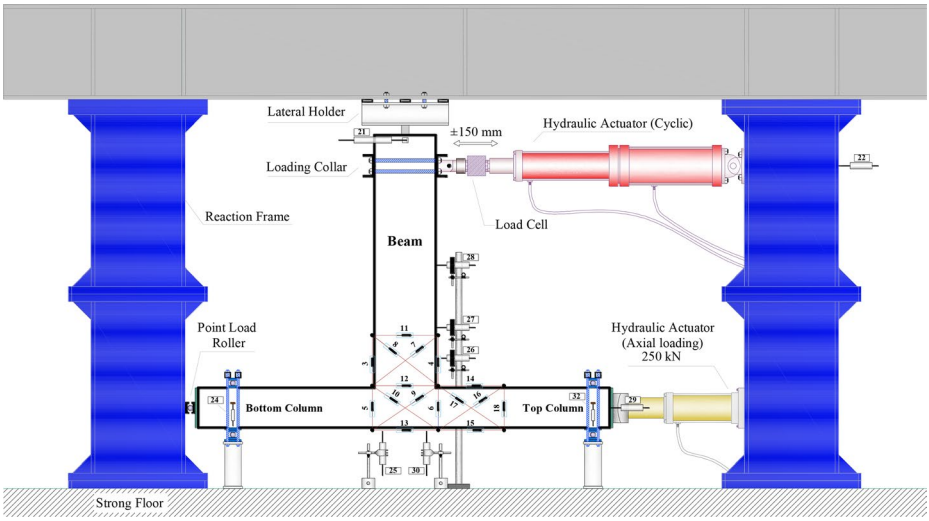

Fig. 3 Typical bare beam-column joint and general setup

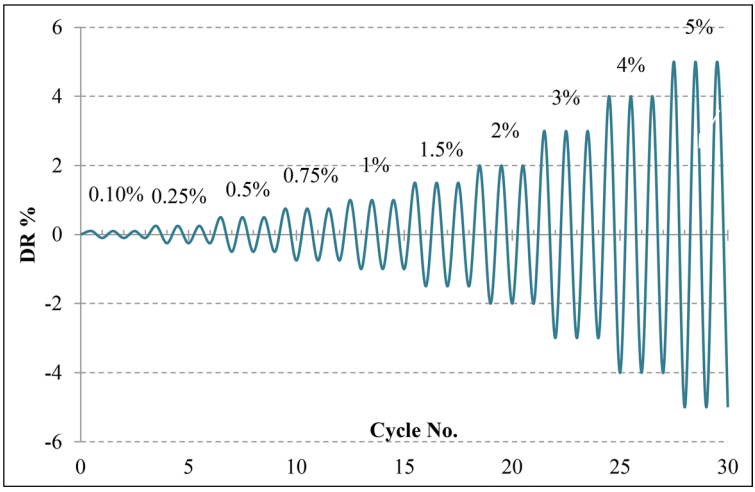

Fig. 4 Cyclic loading protocol used to test the joints

2.4 Core repair/recast and PTMS strengthening strategy

As the initial tests damaged extensively the core, the damaged concrete was completely removed (Fig. 6a) and the core was repaired (recast) with new highly-workable concrete (Fig. 6b). After the new concrete set, the edges of the core and columns were rounded off to a radius of 20 mm using a grinder. This was done to prevent concentration of stresses and potential rupture of the external PTMS at sharp corners. It should be noted that whilst epoxy resin injection (e.g. Li et al. 2012; Sasmal et al. 2011; Beydokhti and Shariatmadar 2016) and concrete cover repairs (Hadi and Tran 2014; Esmaeeli et al. 2015) can be sufficient to

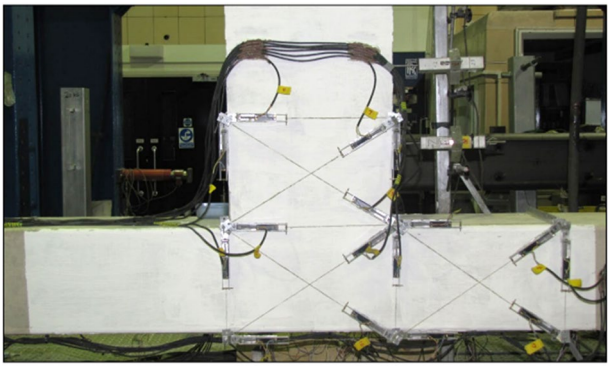

Fig. 5 Typical view of potentiometers and some LVDTs, bare joint JC-1

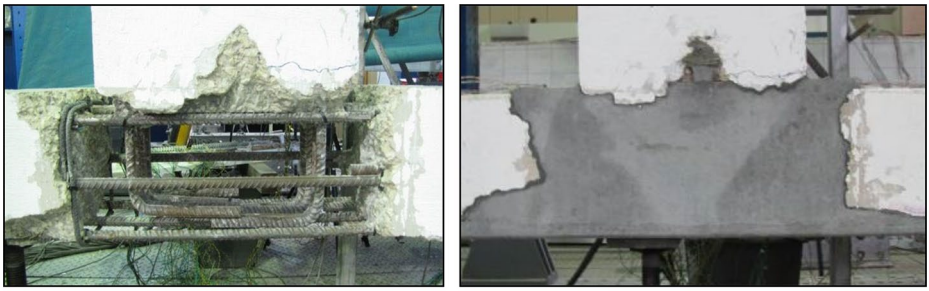

(a) (b)

Fig. 6 Typical repair of core zone of joints after initial tests, joint JC-1 (**a**) view of core zone after removal of damaged concrete, and (**b**) view of core zone after repair/recast with new concrete

repair slightly or moderately damaged joints, in the case of severe damage a core replacement is often necessary (e.g. Ghobarah and Said 2001, 2002; Garcia et al. 2014a). It should be noted that in severely damaged RC buildings, the removal and recast of the concrete core would require the use of temporary shoring near the joint zone. Shoring can be removed after the recast core sets, thus allowing the installation of PTMS strengthening.

Three concrete mixes were used to recast the joints. The mixes were produced using the following proportions: Ordinary Portland Cement = 315 kg/m^3, pulverised fly ash = 135 kg/m^3, fine aggregate 0–4 mm = 7 35 kg/m^3), 10 mm coarse aggregate = 935 kg/m^3, and water = 180 kg/m^3. Plasticiser was also added to the new highly-workable concrete mixes (2.5 kg/m^3 for JA-3, JB-1 and JC-1; 5.0 kg/m^3 for JA-1). The above mix design led to strengths of 39.3 to 57.0 MPa, as reported in Table 1. The new concrete of joint JA-1PTMS also had 50 kg/m^3 of recycled tyre steel fibers. This produced a high-strength steel fibre reinforced concrete (SFRC) with f_{cm}=85.0 MPa, as reported in Table 1. Short recycled steel fibres recovered from post-consumer tyres (Graeff et al. 2012; Alsaif et al. 2019) were used in an attempt to limit the crack width in the core during subsequent tests. The steel fibres had a mean diameter of 0.2 mm and a variable length (90% of the fibres had length in the range between 3 and 22 mm). The SFRC mix also contained 5 kg/m^3 of superplasticiser to enhance workability. The core zones of joints JA -3PTMS, JC-1PTMS and JB-1PTMS were

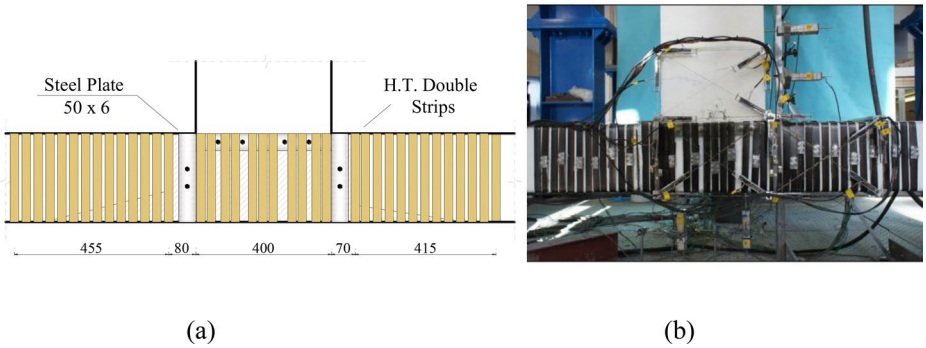

Fig. 7 Strengthening strategy adopted for joint JC-1PTMS (**a**) schematic view, and (**b**) actual strengthed joint

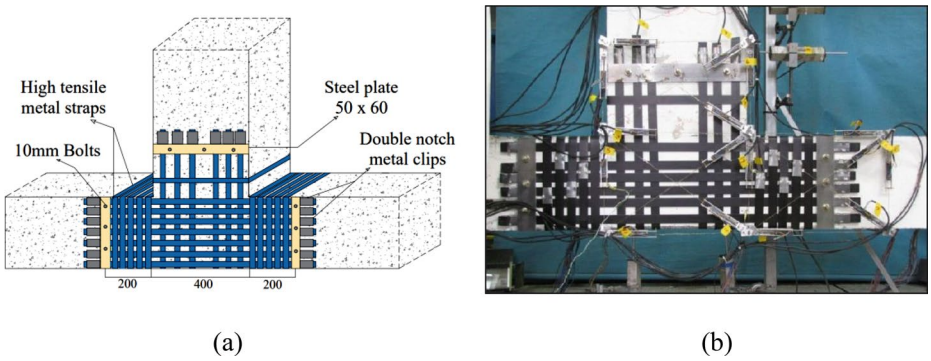

Fig. 8 Strengthening strategy adopted for joint JA-1PTMS (**a**) schematic view, and (**b**) actual strengthened joint

recast with normal highly-workable concrete with 2.5 kg/m^3 of superplasticiser (f_{cm}=39.3 to 57.0 MPa in Table 1).

Following the repair/recast of the core with new concrete, all joints were strengthened with different PTMS strengthening strategies. The main strengthening goal was to increase the shear capacity of the joints. The metal straps were post-tensioned to approximately 30–40% of their yield strength using pneumatic tools. The amount and layout of metal straps was selected based on the assumption that the metal straps can be treated as conventional tensile reinforcement, according to the design methodology presented by Garcia et al. (2014a). Appendix A includes design calculations for joint JC-1PTMS, whereas Fig. 7a shows schematically the PTMS strengthening strategy adopted for this joint.

2.4.1 JA-1PTMS

This joint was strengthened using one layer of metal straps in the horizontal and vertical directions on each face of the joint, as shown in Fig. 8a. The straps extended 200 mm into the beam and columns away from the core zone. The tensioning in the straps was done from one end of the straps, whilst the other end was anchored with metal seals against metal

plates (50×60×6 mm thick). The plates were fixed to each face of the joint using six 10 mm diameter bolts inserted in holes prefilled with epoxy adhesive mortar. Figure 8b shows joint JA-1PTMS before the second test and typical instrumentation.

2.4.2 JC-1PTMS

In this joint, a ⊓-shaped steel plate (6 mm thick) was fixed on each face of the core to hold two layers of straps (Fig. 9a). The plates were fixed using six 10 mm diameter bolts inserted in holes prefilled with epoxy adhesive mortar. After the mortar set, the plates were partially tightened with nuts and washers leaving a small gap of approximately 1 mm between the plates and the concrete faces. This was necessary to enable the two-layer metal straps to pass through and be secured. Additional straps confined the column at each side of the core. Figure 9b shows joint JC-1PTMS.

2.4.3 JA-3PTMS and JB-1PTMS

The strengthening strategy of these joints (Fig. 10a) consisted of confining straps around the beam and column (see straps ① and ② in Fig. 10b). Additionally, two sets of diagonal straps were fixed around the joint core (straps ③ and ④ in Fig. 10b), and these reacted against three crank-shaped steel plates: two L-shaped plates on top of the column (Detail 1 in Fig. 10b), and one plate at the back of the core zone (Detail 2 in Fig. 10b). This was done to avoid drilling the joint to fix the steel bolts and PTMS were also installed on the column zone near the core to enhance the bond strength of the spliced bars. In addition, in joint JB-1PTMS, the straight longitudinal beam bars were welded to the column bars to prevent premature pullout failures. Figure 10c shows joint JB-1PTMS.

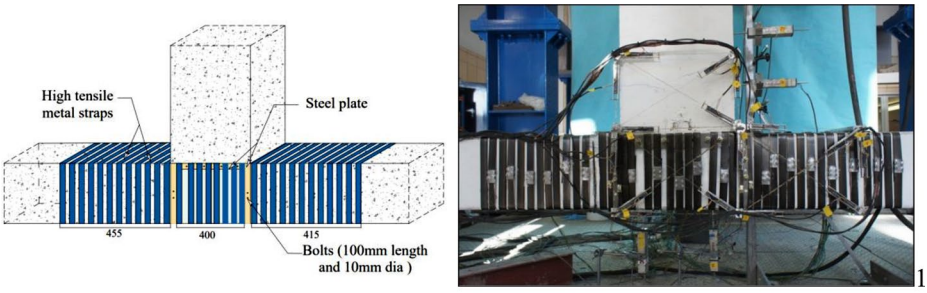

Fig. 9 Strengthening strategy adopted for joint JC-1PTMS (**a**) schematic view, and (**b**) actual strengthed joint

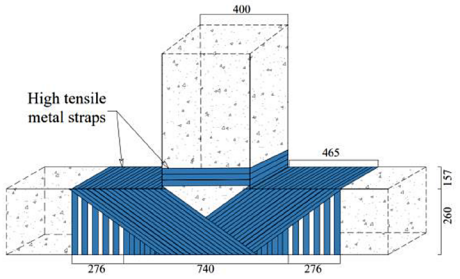

(a)

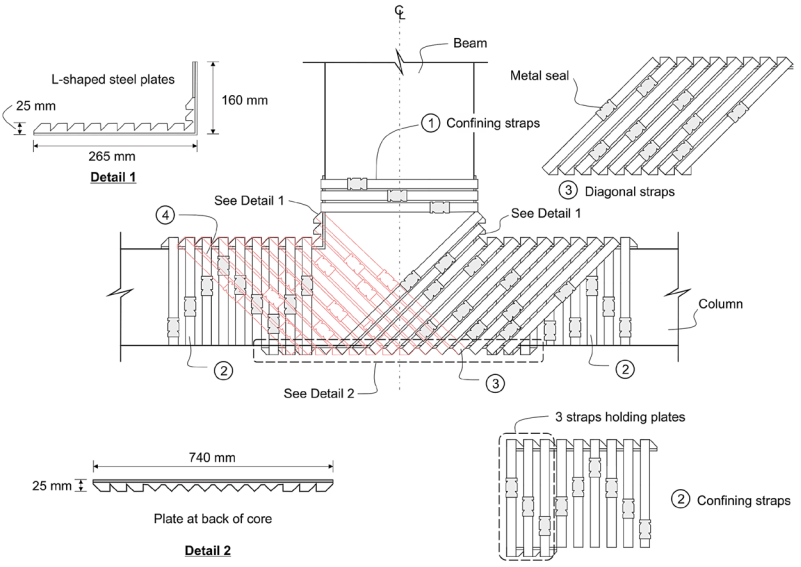

(b)

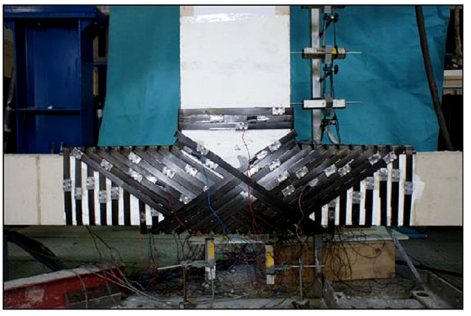

(c)

Fig. 10 Strengthening strategy adopted for joints JA-3PTMS and JB-1PTMS (**a**) schematic view, (**c**) details of steel plates and diagonal configuration of straps, and (**c**) actual joint JB-1PTMS

3 Test results and discussion

3.1 Damage on bare and PTMS-strengthened joints

The initial cycles (DR ± 0.5%) did not cause any evident cracking on the bare jonts. A sudden drop in capacity occurred when the first diagonal crack formed in the core at DR ± 1.5%. This drop occurred in the pull direction when the bottom beam bars were in tension. The load and DR at the onset of diagonal cracking were similar for all bare joints, regardless of the type of detailing in the longitudinal beam reinforcement. Diagonal cracks formed and widened in the core zone as the DR increased progressively during the tests. At large drift ratios (DR ± 4%), concrete spalling ocurred in the core zone. Figs. 11a-b show typical damage observed in two joints after the initial tests on the bare joints. All bare joints failed due to excessive shear cracking in the core zone, accompanied by compressive failure of the diagonal struts in the core zone (J-type failure).

Damage in the PTMS-strengthened joints was more difficult to observe because the metal straps covered most of the core. However, at DR ± 1%, ± 1.5%, ± 2% and ± 3%, the cracks that formed during the initial tests on the bare joints re-opened, and new cracks formed at the old and new concrete interfaces. Figure 12a-d show the damage experienced by the PTMS-strengthened joints at the end of the tests after removing the metal straps. The PTMS-strengthened joints failed due to gradual shear cracking in the core accompanied by damage and cracking in the beam (JB-type failure), with the exception JA-1PTMS where the beam had no visible damage. All columns had some flexural cracks near the core, but there was no evidence of lap splice failure in the longitudinal bars.

3.2 Load-drift response of bare and PTMS-strengthened joints

Figure 13a compares the load-drift responses of joints JA-1 and JA-1PTMS. Due to an issue with the testing controls, joint JA-1 was subjected to only one loading cycle in the post-peak stage. The capacities were + 40.4 kN (push direction) and − 45.1 kN (pull direction), corresponding to DR + 1.14% and DR -2.03%, respectively. Conversely, the capacities of joint JA-1PTMS were + 75.5 kN and − 65.6 kN in the push and pull directions, respectively, which occurred at a DR ± 2%. The tests were halted due to the rupture of the metal seals that

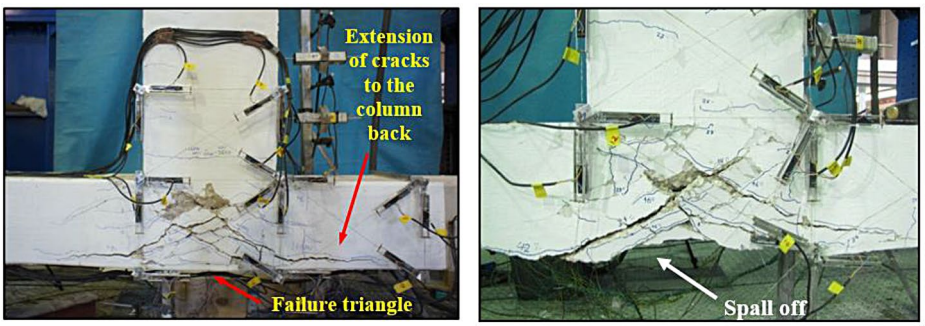

Fig. 11 Typical damage of bare joints: (**a**) JA-3, and (**b**) JC-1

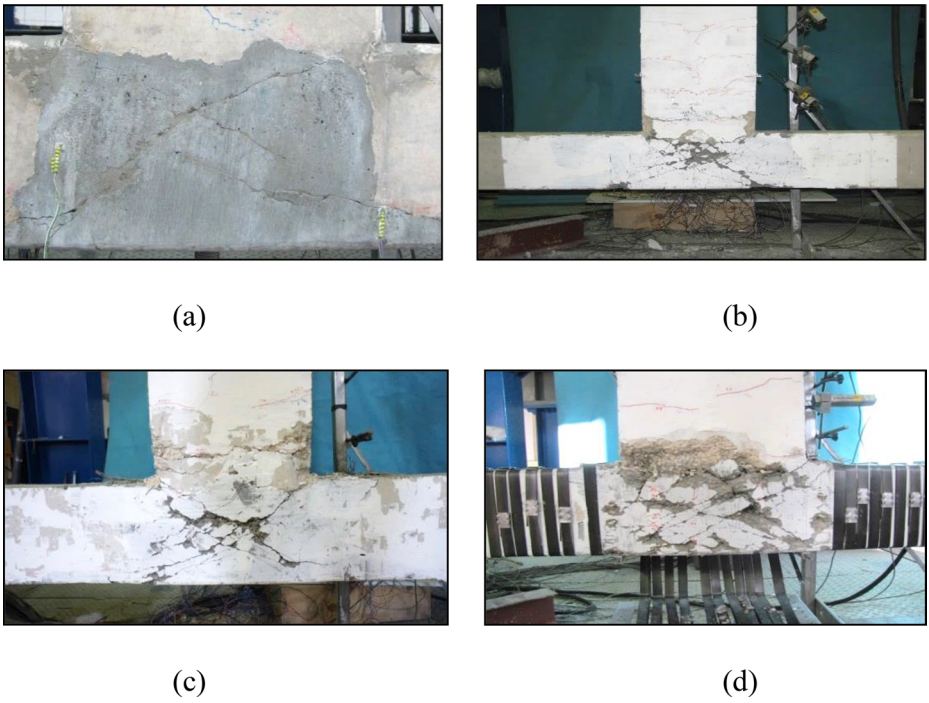

Fig. 12 Damage of PTMS-strengthened joints, (**a**) JA-1PTMS (**b**) JA-3PTMS (**c**) JB-1PTMS, and (**d**) JC-1PTMS

were anchored on the steel plates. Table 2 summarises the load capacities and corresponding drift ratios of the bare and PTMS-strengthened joints in both loading directions.

The load-drift responses of joints JA-3 and JA-3PTMS are compared in Fig. 13b. The capacities of JA-3 were +58.7 kN and −51.9 kN at DR+1.51% and −1.52%, respectively. After a DR±4%, the load dropped below 50% of the maximum capacity. The response of joint JA-3PTMS shows that the capacities in the push and pull directions were +75 kN and −69 kN, respectively, at a DR±2%. Compared to the bare joint JA-3, JA-3PTMS had 30% and 20% higher capacity in the push and pull directions, respectively. However, premature debonding of the longitudinal beam bars of JA-3PTMS occurred, which hindered reaching higher loads in this joint.

The responses of joints JB-1 and JB-1PTMS are compared in Fig. 13c, whereas Fig. 13d compares the responses of JC-1 and JC-1PTMS. The results in these figures and the data in Table 2 confirm the effectiveness of the adopted core repair/recast and PTMS strengthening strategies at improving the capacity of these joints. For instance, compared to joint JB1, the capacity of JB-1PTMS was 72% and 95% higher in the push direction and pull directions, respectively (Fig. 13c). Similarly, the DR at maximum capacity increased by an average of 150% considering both directions.

In comparison to JC1, JC-1PTMS had 87 kN and 64 kN capacities in both the push direction (+75%) and pull directions (+34%), as shown in Fig. 13d; Table 2. It should be noted that the different capacity between the push and pull directions of JC-1PTMS in Fig. 13d was due to a malfunction of the test equipment. Indeed, a sudden large displacement dur-

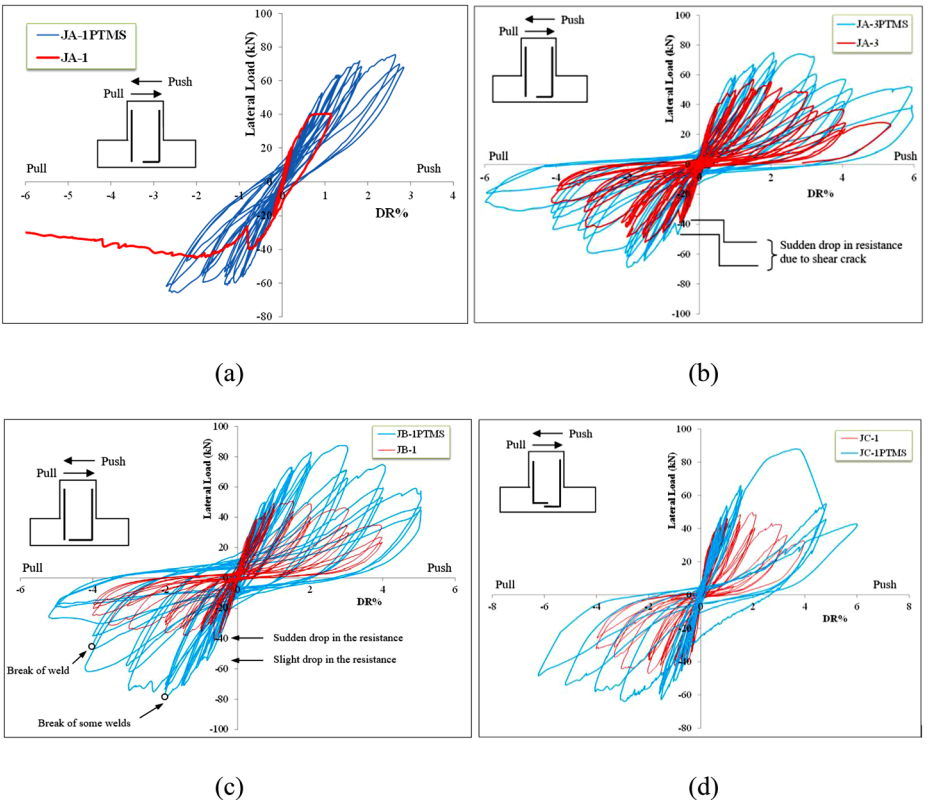

Fig. 13 Load-drift response of bare and PTMS-strengthened joints (**a**) JA-1 & JA-1PTMS, (**b**) JA-3 & JA-3PTMS, (**c**) JB-1 & JB-1PTMS, and (**d**) JC-1 & JC-1PTMS

Table 2 Maximum load capacities and corresponding drift ratios (DR) of tested joints

Joint	JA-1		JA-3		JB-1		JC-1	
Direction	F (kN)	DR (%)	F (kN)	DR (%)	F (kN)	DR (%)	F (kN)	DR (%)
Push (+)	40.4	1.14	55.7	1.51	50.8	1.54	49.6	1.97
Pull (-)	-45.1	-2.03	-51.9	-1.52	-41.1	-0.64	-47.7	-1.44
Joint	**JA-1PTMS**		**JA-3PTMS**		**JB-1PTMS**		**JC-1PTMS**	
Direction	F (kN)	DR (%)	F(kN)	DR (%)	F (kN)	DR (%)	F (kN)	DR (%)
Push (+)	75.5	2.00	75	2.08	87.4	2.90	86.7	3.34
Increase	87%	76%	35%	38%	72%	89%	75%	69%
Pull (-)	-65.6	-2.00	-69	-2.01	-80	-2.00	-64.1	-2.92
Increase	45%	1%	33%	32%	95%	211%	34%	41%

ing the last cycle at DR = + 1.5% caused significant damage to the joint, thus affecting the results. The results in Figs 13b-d also show that the repair/recast and PTMS strengthening were effective at increasing the deformation capacity of some joints. This is particularly evident in JC-1PTMS, where the ultimate DR increased by approximately 50% from DR ± 4% to DR ± 6% in both push and pull directions. Overall, the experimental results indicate that

the capacity of the bare joints was approximately 50% that of their theoretical plastic capacity. Following the repair/recast and PTMS strengthening, joint JB-1PTMS showed the highest capacity enhancement of all tested joints. This suggests that the welding used in this joint prevented the premature debonding observed in the longitudinal beam bars of JA-3PTMS. Joint JA-1PTMS and JA-3PTMS had similar performance despite the difference in concrete quality and axial load.

3.3 Cumulative energy

Figs. 14a-b compare the cumulative energy dissipated by the bare and PTMS-strengthened joints at different DRs. The cumulative energy was calculated by summing up the energy dissipated in the load-displacement cycles throughout the full test. Since it was not possible to calculate the energy of joint JA-1 due to issues during testing, the results are not presented in Fig. 14a. The results in Fig. 14a show that most of the energy absorption occurred during the first cycle of the last two DRs (±3% and ±4%), when large deformations and severe loss in stiffness took place. By the end of the test (DRs±4%) and despite the different detailing of reinforcement at the core, joints JA-3, JB-1 and JC-1 had dissipated similar cumulative energies of 9.6 kNm, 9.2 kNm and 8.0 kNm, respectively. Conversely, Fig. 14b shows that the PTMS-strengthened joints JA-3PTMS, JB-1PTMS and JC-1 PTMS dissipated the much high cumulative energies of 26.3 kNm, 34.0 kNm and 15.7 kNm at DR of ±6%, respectively. It should be noted that the bare and PTMS-strengthened joints dissipated similar amounts of energy up to a DR of ±2% (i.e. before wide shear cracks developed in the core zone). It is also evident that the energy dissipation of the PTMS-strengthened after that DR increased significantly as cracking and damage progressed. However, at a common DR of ±4%, the PTMS-strengthned joints dissipated up to 2.7 times more energy compared to bare counterparts. The test results also indicate that, at the end of the tests, the PTMS-strengthed joints dissipated up to 3.7 times the energy dissipated by the bare joint (compare JB-1PTMS vs. JB-1). This indicates that the repair and PTMS strengthening strategies were very effective at improving the energy dissipation capacity of the originally substandard joints.

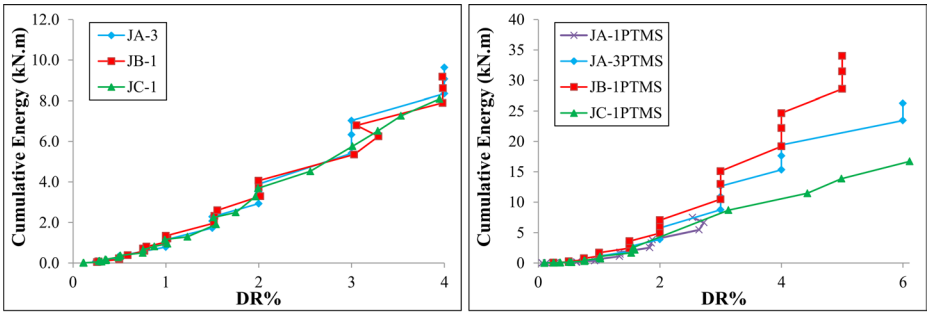

Fig. 14 Cumulative energy dissipated by (**a**) bare joints, and (**b**) PTMS-strengthened joints

3.4 Contributions of repair/recast and PTMS to total joint shear strength

The results reported in Table 1 include the combined contributions of the repair/recast core and the PTMS strengthening. To calculate the actual contribution of the PTMS strengthening to the shear capacity of the joints, it is necessary to decouple the effect of the core repair/recast. Table 3 compares the experimental horizontal shear stress $\upsilon_{j,max}$ (calculated using Eq. 1) and the corresponding shear strength factor γ (where $\gamma=\upsilon_{j,max}/\sqrt{f_{cm}}$) of the tested joints. Table 3 also includes the factor γ calculated according to the approaches proposed by Hassan for J-type failure 'γ_{HJ}' (Hassan 2011), Park and Mosalam 'γ_{PM}' (Park and Mosalam 2012, 2013), and ASCE/SEI 41–17 'γ_{A41}' (ASCE 2017). Note that the values γ reported in Table 3 are the average of the push and pull directions.

$$\upsilon_{jh} = V_{jh} \Big/ A_j \tag{1}$$

where V_{jh} is the maximum shear force resisted by the joint; and A_j is the area of the joint core.

Table 3 shows that the bare joints have very similar shear strength factors γ ranging from 0.49 to 0.52. The results also indicate that ASCE/SEI 41–17 predicts accurately (within a 5% accuracy) the actual shear capacity of the substandard bare joints (see factor γ_{A41}). Therefore, a value $\gamma=0.5$ as is used in this study to calculate the shear capacity of the recast core in the PTMS-strengthened joints (see values $\upsilon_{j,\,core}$ in Table 3). Accordingly, the contribution of the PTMS strengthening to the total shear capacity of a PTMS-strengthened joint is calculated as $\upsilon_{j,\,PTMS}=\upsilon_{j,\,max}-\upsilon_{j,\,core}$. It should be noted that past research (e.g. Garcia et al. 2014a; Hung et al. 2022) also found that ASCE/SEI 41–17 was accurate at prediciting the shear capacity of other substandard beam-column joints. Therefore, ASCE 41–17 can be used to provide conservative predictions of the capacity of substandard joints as those tested in this study.

The last two columns of Table 3 show the decoupled shear capacity enhancements attributed to the repair/recast core ($\Delta\upsilon_{j,\,core}$) and PTMS strengthening ($\Delta\upsilon_{j,\,PTMS}$) of the PTMS-strengthened joints. The results indicate that the repair/recast of the core zone was very effective at increasing the shear capacity of the joints by up to 42% (JB-1PTMS), while the PTMS strengthening increased further the capacity by up to 25% (JA-3PTMS). Based on these results, it is evident that the strengthening strategies adopted for joints JA-3PTMS and JB-1PTMS were more effective in achieving the strengthening goal. Also, additional inter-

Table 3 Shear strength contributions of core repair/recast and PTMS strengthening

ID	$\upsilon_{j,\,max}$ (MPa)	γ	γ_{HJ}	γ_{PM}	γ_{A41}	$\upsilon_{j,\,core}$ (MPa	$\upsilon_{j,\,PTMS}$ (MPa)	$\Delta\upsilon_{j,\,core}$ (%)	$\Delta\upsilon_{j,\,PTMS}$ (%)
JA-1	2.32	0.49	0.75	1.19	0.5	-	-	-	-
JA-3	2.92	0.52	0.75	1.00	0.5	-	-	-	-
JB-1	2.69	0.50	0.75	1.05	0.5	-	-	-	-
JC-1	2.64	0.49	0.75	1.05	0.5	-	-	-	-
JA-PTMS	3.91	-	-	-	-	3.13	0.78	+16	+25
JB-PTMS	4.55	-	-	-	-	3.75	0.80	+42	+21
JC-PTMS	4.10	-	-	-	-	3.77	0.32	0	+9

ventions such as welding of longitudinal beam bars at the core zone of JB-1PTMS proved very effective in preventing premature bond failure of short anchored reinforcement.

4 Modelling of bare and ptms-strengthend beam-column joints

4.1 General geometry and scissors model

In this study, DRAIN-2DX software was used to model the joints and to provide further insight into their behaviour. Past studies have demonstrated the effectiveness of DRAIN-2DX at simulating the nonlinear behaviour of structures (e.g. Seif-eddine et al. 2019, Elfath et al. 2021). Fig. 15a shows the model of a typical joint in DRAIN-2DX. A pinned support at the bottom of the column restrained vertical and horizontal movements. Axial column shortening was allowed through a top vertical roller. Outside the core zone, the beam and column were modelled using Element15 (E15) that simulates concrete and steel bars as discrete fibres. Element15 is a distributed plasticity element that considers the P-M interaction automatically. Fig. 15a shows the cross sections of the discretised beam and column. The experimentally determined material properties were used for the concrete and steel fibres.

In this study, a "scissors model" is used to model the panel zone. The model consists of a rotational spring with rigid links extending along the core dimensions. Past studies used a similar approach to simulate the behaviour of beam-column joints (e.g. Sharma et al. 2011; Birely et al. 2012; Amirsardari et al. 2019 Kolozvari et al. 2023). As shown in Fig. 15b, the core zone was modelled using two rigid link elements spanning along the core dimensions, and one nonlinear rotational spring embedded in the connecting node of the rigid elements. Two translational nonlinear springs were embedded at the column/core interfaces.

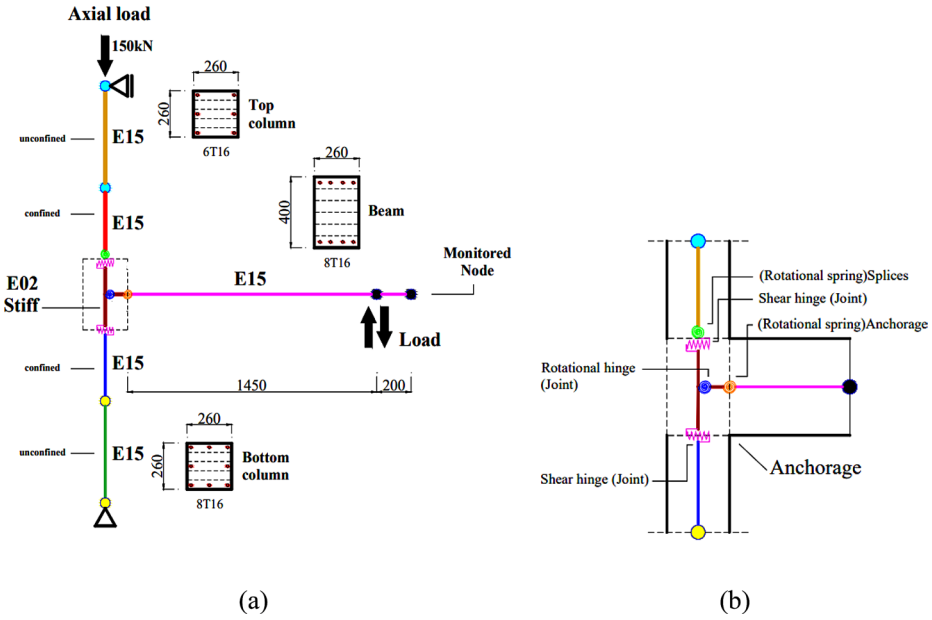

Fig. 15 DRAIN-2DX model (**a**) beam-column joint model, and (**b**) core zone "scissors model"

The beam moment (M_b) vs. shear deformation of joint (Δ_j) relationship obtained from the tests was used to model the rotational spring. Likewise, the joint horizontal shear force (V_j) vs. shear deformation ($\Delta_c = \Delta_j \cdot h_b / 2$, where h_b is the beam hight) relationship was used to model the column portion of the joint. Accordingly, the M_b- Δ_j and V_j - Δ_c relationships were extracted from the experimental results of each bare and PTMS-strengthened joint tested in this study, and such values were used as inputs in the rotational and translational springs shown in Fig. 15b. As a result, the contribution of the different PTMS strengthening strategies is implicitly accounted for in the input values. Element02 (E02) with a large value of stiffness was adopted to model the rigid joint elements of the scissors model.

4.2 Bar slippage deformations

Slip deformations are included in the model as moment-rotation relationships. To achieve this, slip deformations were first transformed into rotations at the beam or joint interface. The cross-section rotation due to bar slippage was assumed to occur about the neutral axis, as shown in Fig. 16. Accordingly, the slip rotation was calculated as the bar slip (measured by LVDTs during the tests) divided by the distance between the neutral axis and the slipping bar (i.e. the width of the open crack), as defined by Eq. 2:

$$\theta_{slip} = \frac{Slip}{d - c} \tag{2}$$

Further details about the approach adopted in the modelling of the bare and PTMS-strengthened joints tested in this study can be found in Helal (2012).

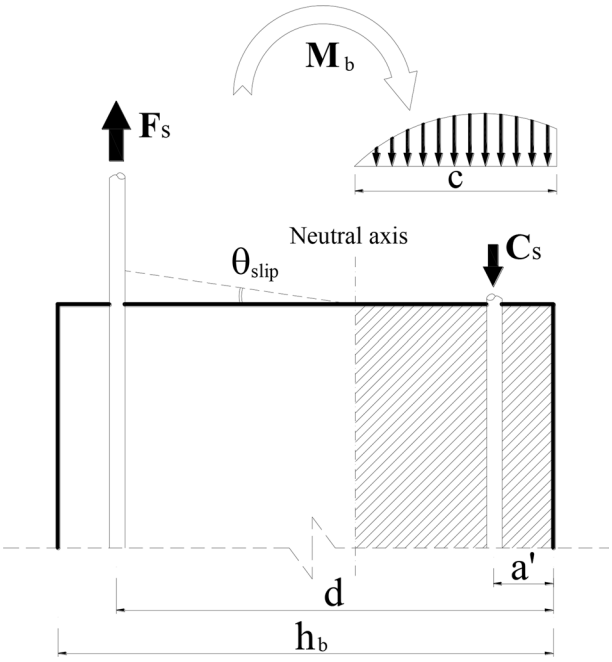

Fig. 16 Calculations of rotations due to bar slippage

After modelling the bare and PTMS-strengthened joints, nonlinear analyses were performed to obtain the corresponding nonlinear load-displacement envelope response, as discussed in the next section. It should be noted the envelope is considered in this study because current guidelines (e.g. ASCE/SEI 41−17) also use envelope responses to model the nonlinear behaviour of beam-column joints.

5 Results & discussion

5.1 Load-displacement envelope response

Figure 17a-c compare the experimental load-displacement response of the bare joints and the numerical results from DRAIN-2DX. The results indicate that the scissors model predicted the first (shear) cracking, initial stiffness, peak strength and post-peak degradation with reasonable accuracy. Likewise, Fig. 18a-c compare the experimental load-displacement response of the bare joints and the numerical results from DRAIN-2DX. The results show that, in general, the scissors model also captured well the load-displacement response of the PTMS-strengthened joints. The scissors model adequately predicts that all joints reach their capacity before plastic hinging develops in the beam. Despite the minor differ-

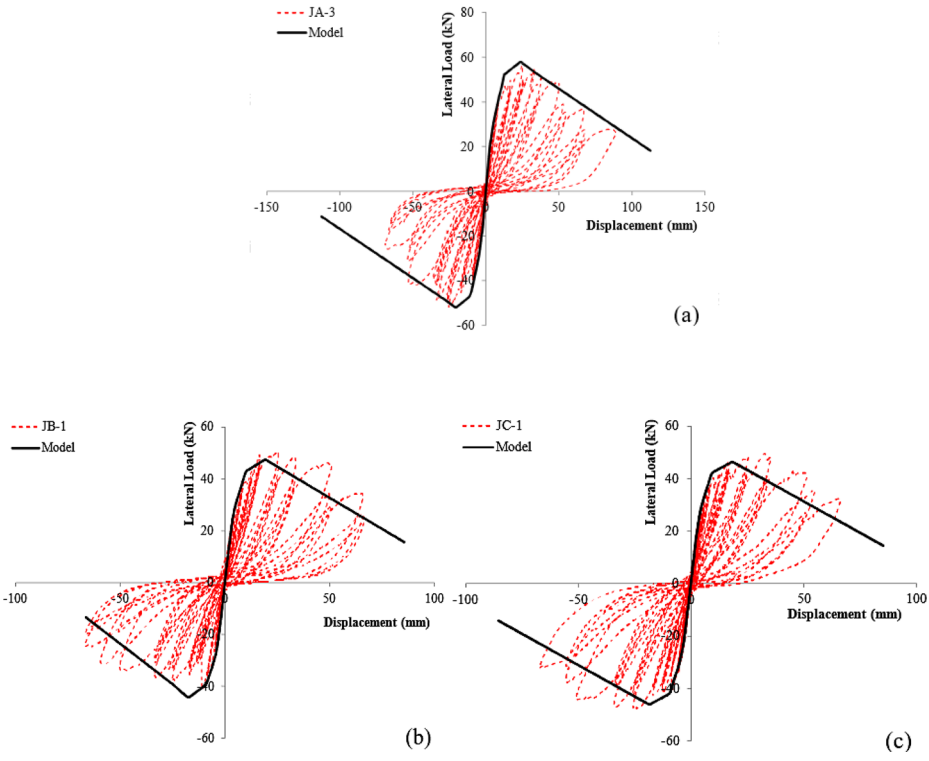

Fig. 17 Comparison of experimental results and DRAIN-2DX predictions for bare joints (**a**) JA-3, (**b**) JB-1, and (**c**) JC-1

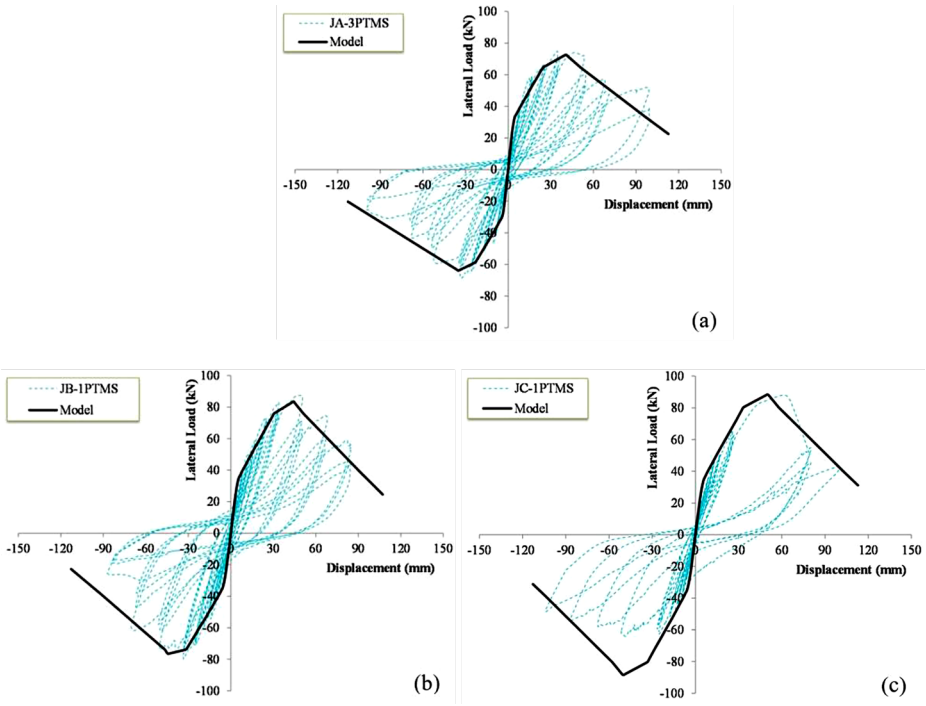

Fig. 18 Comparison of experimental results and DRAIN-2DX predictions for PTMS-strengthened joints (**a**) JA-3PTMS (**b**) JB-1PTMS, and (**c**) JC-1PTMS

ences, it is concluded that the scissors model as used in this study can be confidently used to obtain the nonlinear load-displacement envelope response of PTMS-strengthened joints

Overall, the experimental and numerical results from this study confirm that the repair and PTMS strengthening strategy was very effective at increasing the capacity of the joints. As a result, PTMS is deemed as a viable strengthening alternative to other traditional techniques, particularly to reduce the vulnerability of RC buildings located in earthquake-prone developing countries. However, in the strengthening of real buildings, the presence of beams and slabs may prevent the installation of the metal straps on the faces of the joints. In these cases, additional steel plates can be used to support the metal straps as proposed by Garcia et al. (2014a), 2017). Due to the small number of joints tested in this study further research is necessary to verify the effectiveness of the PTMS technique on different joints with different geometries and strengthening strategies. Moreover, more practical design aids (e.g. Ma et al. 2015, 2016a; Imjai et al. 2017) are also necessary. Whilst the scissors model in DRAIN-2DX proved effective to model the shear behaviour of the bare and PTMS-strengthened joints, other software (e.g. OpenSees) and modelling approaches should also be explored to provide further insight into the hysteretic behaviour of PTMS-strengthened joints.

6 Summary and conclusions

This article presents an in-depth exploration of the seismic performance of exterior reinforced concrete (RC) beam-column joints, with a focus on their strengthening using Post-Tensioned Metal Straps (PTMS), a novel technique offering active confinement. The study involved a two-stage experimental and numerical investigation. In the initial phase, four substandard joints underwent reverse cyclic loading, resulting in substantial core zone damage. Subsequently, the damaged core was repaired with new concrete, and the joints were reinforced with PTMS, followed by a repetition of cyclic tests. The results were analysed and compared to predictions derived from existing models in the literature. Additionally, the joints were numerically modeled using the DRAIN-2DX software, adopting a "scissors model" to determine their nonlinear envelope response.The following key conclusions emerge from the test results and analysis presented in this article:

- **Bare Joint Behaviour**: The behaviour of the substandard bare joints was characterised by extensive cracking and damage in the core, ultimately leading in premature shear failure (J-type). The capacity of the bare joints was approximately 50% that of their theoretical plastic capacity.
- **ASCE/SEI 41–17 Predictions**: ASCE/SEI 41–17 predicts the strength factor γ of the substandard bare joints within a 5% accuracy. This confirms that the ASCE/SEI 41–17 can be reliably used to provide conservative predictions of the capacity of substandard joints as those tested in this study.
- **Core Recasting and PTMS Strengthening**: Repairing by recasting the core with new concrete led to a substantial increase in the shear capacity of the joints, with improvements of up to 42% compared to their original bare counterparts. These results suggest that even the recasting of the (damaged) core zone with new concrete could be a potential cost-effective option to improve the behaviour of damaged beam-column joints, particularly if limited resources for structural strengthening with PTMS are available. Subsequent PTMS strengthening of the recast core further enhanced the capacity by up to 25%. Furthermore, the repair and PTMS strengthening proved effective in significantly increasing the deformation capacity of joint JC-1PTMS, achieving an enhancement of approximately 50%.
- **Model Validation**: Results from DRAIN-2DX software confirm the efficacy of that scissors model in accurately simulating the nonlinear load-displacement envelope response of both bare and strengthened joints. Hence, the scissors model can be confidently used to obtain the nonlinear load-displacement envelope response of PTMS-strengthened joints as those tested in this study.

This article makes a significant contribution to advancing the use of PTMS as an innovative and cost-effective technique for the strengthening of beam-column joints, thus making it an attractive option compared to traditional strengthening techniques. The results from this study suggest that the PTMS technique can offer a practical solution to reduce the vulnerability (and thus the seismic risk) of substandard RC buildings, particularly in developing countries with limited financial resources.

7 Appendix A

For illustration, the PTMS design is shown for joint JC-1 PTMS.

The horizontal shear force demand in the joint (V_{jh}) was computed using force equilibrium according to Equation (A1),

$$V_{jh} = T_b - V_{col} = P\left[\frac{L_b}{z} - \frac{L_b + 0.5h_c}{H_c}\right] = 150 \times 10^3\left[\frac{1400}{0.875\,(368)} - \frac{1400 + 0.5\,(260)}{2400}\right] = 556kN \quad (3)$$

where T_b is the tension force of the top beam reinforcement; V_{col} is the column shear force; L_b is the beam length to the applied at the loading point; H_c is the distance between column supports; h_c is the height of the column cross section; and z is the lever arm of the beam flexural moment (assumed equal to 0.875 the beam effective depth).

The PTMS strengthening was designed considering the total shear capacity of the joint core as the sum of concrete and PTMS contributions. The concrete contribution (V_c) was computed according to ASCE/SEI 41–17 (2017) guidelines using Equation a shear strength coefficient

$$\gamma = 0.083 \times 8\sqrt{f_{ck}} = 0.664\sqrt{f_{ck}} \quad (4)$$

The strength of the new concrete core of joint JC-1PTMS using the equation below,

$$V_{cc} = \gamma A_j \sqrt{f_{ck}} = (0.664)\,(260 \cdot 260)\sqrt{57} = 339kN \quad (5)$$

where A_j is the effective horizontal joint area.

The shear resistance provided by the horizontal metal straps (V_s) was then calculated using first principles and considering the straps as an additional shear reinforcement (see Eq. 3). In this example, it is assumed that two-layered metal straps are spaced at $s = 50$ mm centre-to-centre, and that the straps are tensioned to 35% of their yield strength. Therefore:

$$V_{sh} = (A_v f_y d_c)/S = ((2)(1.27)(25)(930)(228))/50 = 269kN \quad (6)$$

where, A_v is the cross-sectional area of the steel straps and dc is the effective depth of the column. The proposed PTMS layout was thus adequate to sustain the design shear force demand in the joint ($V_{cc} + V_{sh} > V_{jh}$).

Acknowledgements The first author thankfully acknowledges the financial support provided by Damascus University (Syria) for his PhD studies. This research work was supported by Walailak University Graduate Research Fund, Contract No. CGS-RF-2023/10. The third author gratefully acknowledges the support from the National Research Council of Thailand (NRCT5-RSA63019-04) for supporting his research in this field. The authors acknowledge the support provided by the Capacity Enhancement and Driving Strategies for Bilateral and Multilateral Cooperation for 2021 (Thailand and UK). This research was financially supported by Wailalak University's Graduate Research Fund contract no. CGS-RF2023/10.

Author contributions ***YH***: Conceptualization, Methodology, Software, Investigation; ***RG***: Conceptualization, Methodology, Software, Validation, Writing - Original Draft, Writing - Review & Editing; ***TI***: Conceptualization, Methodology, Formal analysis, Validation, Writing - Original Draft, Writing - Review & Editing, Visualization; ***PA***: Writing - Original Draft, Visualization; ***MG***: Supervision; ***KP***: Conceptualization, Supervision, Writing - Review & Editing.

Data availability The data generated and analysed during the current study are available from the first author on reasonable request.

Declarations

Competing interests The authors have no relevant financial or non-financial interests to disclose.

References

Abdullah W (2023) Shear strengthening of normal steel reinforced concrete beams using post-tensioned metal straps fully wrapped around the beams. Adv Struct Eng 26(9):1636–1646. https://doi.org/10.1177/1369433223117425

Abou-Elfath H, Ramadan M, Elhout E (2021) Evaluating the ductility reduction factors of SDOF self-centering earthquake-resisting structural systems. Bull Earthq Eng 19(3):1605–1624. https://doi.org/10.1007/s10518-021-01041-z

Alsaif A et al (2018) October., Fatigue performance of flexible steel fibre reinforced rubberised concrete pavements, Eng. Struct., vol. 193, no. pp. 170–183, 2019, https://doi.org/10.1016/j.engstruct.2019.05.040

Amirsardari A, Rajeev P, Lumantarna E, Goldsworthy HM (2019) Suitable intensity measure for probabilistic seismic risk assessment of non-ductile Australian reinforced concrete buildings. Bull Earthq Eng 17(7):3753–3775. https://doi.org/10.1007/s10518-019-00632-1

ASCE/SEI 41–17 (2017) Seismic evaluation and retrofit of existing buildings. American Society of Civil Engineers, Reston, Virginia

Bindhu KR, Jaya KP (2010) Strength and behaviour of exterior beam column joints with diagonal cross bracing bars. Asian J Civ Eng 11(3):397–410

Bindhu KR, Mohana N, Sivakumar S (2016) New reinforcement detailing for concrete jacketing of Non-ductile Exterior Beam–Column joints. J Perform Constr Facil 30(1):1–9. https://doi.org/10.1061/(asce)cf.1943-5509.0000700

Birely AC, Lowes LN, Lehman DE (2012) A model for the practical nonlinear analysis of reinforced-concrete frames including joint flexibility. Eng Struct 34:455–465. https://doi.org/10.1016/j.engstruct.2011.09.003

BSI BS EN 12390- 6:2009 testing hardened concrete part 6: tensile splitting strength of test specimens, British Standards Institution, London

BSI BS EN 12390-3:2009 testing hardened concrete part 3: compressive strength of test specimens, 2009a, British Standards Institution, London

Seif-eddine C, Chourak M, Abed M, Pujades L (2019) Seismic evaluation method for existing reinforced concrete buildings in North of Morocco. Bull Earthq Eng 17(7):3873–3894. https://doi.org/10.1007/s10518-019-00643-y

Chin CL, Ma CK, Awang AZ, Omar W, Kueh ABH (2018) Stress–strain evaluation of steel-strapped high-strength concrete with modified self-regulating end clips. Struct Concr 19(4):1036–1048. https://doi.org/10.1002/suco.201700134

Choudhury AH, Laskar AI (2021) Rehabilitation of substandard beam-column joint using geopolymer. Eng Struct 238:112241. https://doi.org/10.1016/j.engstruct.2021.112241

Dang CT, Dinh NH (2017) Experimental Study on Structural Performance of RC Exterior Beam-Column Joints Retrofitted by Steel Jacketing and Haunch Element under Cyclic Loading Simulating Earthquake Excitation, Adv. Civ. Eng., vol. no. i, 2017, https://doi.org/10.1155/2017/9263460

Elsouri A, Harajli M (2015) Repair and FRP strengthening of earthquake-damaged RC shallow beam-column joints. Adv Struct Eng 18(2):237–249. https://doi.org/10.1260/1369-4332.18.2.237

Esmaeeli E et al (2015) Retrofitting of Interior RC beam-column joints using CFRP strengthened SHCC: cast-in-place solution. Compos Struct 122:456–467. https://doi.org/10.1016/j.compstruct.2014.12.012
Frangou M, Pilakoutas K, Dritsos S (1995) Structural repair/strengthening of RC columns. Constr Build Mater 9(5):259–266. https://doi.org/10.1016/0950-0618(95)00013-6
Garcia R, Hajirasouliha I, Pilakoutas K (2010) Seismic behaviour of deficient RC frames strengthened with CFRP composites. Eng Struct 32(10):3075–3085. https://doi.org/10.1016/j.engstruct.2010.05.026
Garcia R et al (2014) Full-scale shaking table tests on a substandard RC building repaired and strengthened with post-tensioned metal straps. J Earthq Eng 18(2):187–213. https://doi.org/10.1080/13632469.2013.847874
Garcia R, Jemaa Y, Helal Y, Guadagnini M, Pilakoutas K (2014a) Seismic strengthening of severely damaged Beam-Column RC joints using CFRP. J Compos Constr 18(2):1–10. https://doi.org/10.1061/(asce)cc.1943-5614.0000448
Garcia R, Pilakoutas K, Hajirasouliha I, Guadagnini M, Kyriakides N, Ciupala MA (2017) Seismic retrofitting of RC buildings using CFRP and post-tensioned metal straps: shake table tests. Bull Earthq Eng 15(8):3321–3347. https://doi.org/10.1007/s10518-015-9800-8
Ghobarah A, Said A (2001) Seismic rehabilitation of beam-column joints using FRP laminates. J Earthq Eng 5(1):113–129. https://doi.org/10.1080/13632460109350388
Ghobarah A, Said A (2002) ' Shear Strengthening of Beam-Column Joints,' Shear strengthening of beam-column joints, vol. 0296, no. October, pp. 881–888
Graeff AG, Pilakoutas K, Neocleous K, Peres MVNN (2012) Fatigue resistance and cracking mechanism of concrete pavements reinforced with recycled steel fibres recovered from post-consumer tyres. Eng Struct 45:385–395. https://doi.org/10.1016/j.engstruct.2012.06.030
Hadi MNS, Tran TM (2014) Retrofitting nonseismically detailed exterior beam-column joints using concrete covers together with CFRP jacket. Constr Build Mater 63:161–173. https://doi.org/10.1016/j.conbuildmat.2014.04.019
Hassan EM (2011) Analytical and Experimental Assessment of Seismic Vulnerability of Beam-Column Joints without Transverse Reinforcement in Concrete Buildings, PhD thesis, University of California, Berkeley, CA
Helal Y (2012) Seismic strengthening of deficient exterior RC Beam-column sub-assemblages using post-tensioned metal strips. Dept. of Civil & Structural Engineering, The University of Sheffield, UK
Helal Y, Garcia R, Pilakoutas K, Guadagnini M, Hajirasouliha I (2016) Strengthening of short splices in RC beams using Post-tensioned Metal Straps. Mater Struct 49:1–2. https://doi.org/10.1617/s11527-014-0481-6
Huang Q, Liu Y, Tian L (2023) Seismic performance of the shear-deficient exterior RC beam-column joints strengthened with PHSW, Eng. Struct., vol. 275, no. PB, p. 115309, https://doi.org/10.1016/j.engstruct.2022.115309
Hung CC, Hsiao HJ, Shao Y, Yen CH (2023) A comparative study on the seismic performance of RC Beam-column joints retrofitted by ECC, FRP, and concrete jacketing methods. J Build Eng 64(105691). https://doi.org/10.1016/j.jobe.2022.105691
Helal Y, Garcia R, Pilakoutas K, Guadagnini M, Hajirasouliha I (2016) Bond of substandard laps in RC beams retrofitted with post-tensioned metal straps. ACI Struct J 113(6):1197–1208. https://doi.org/10.14359/51689021
Imjai T, Chaisakulkiet U, Garcia R, Pilakoutas K (2018) Strengthening of RC members using Post-tensioned Metal Straps: state of the research. Lowland Tech Int 20(2):109–118
Imjai T, Setkit M, Garcia R, Figueiredo FP (2020a) Strengthening of damaged low strength concrete beams using PTMS or NSM techniques. Case Stud Constr Mater 13:e00403. https://doi.org/10.1016/j.cscm.2020.e00403
Imjai T, Setkit M, Garcia R, Sukontasukkul P, Limkatanyu S (2020b) Seismic strengthening of low strength concrete columns using high ductile metal strap confinement: a case study of kindergarten school in northern Thailand. Walailak J Sci Technol 17(12):1335–1347
Kalogeropoulos GI, Tsonos ADG, Konstandinidis D, Tsetines S (2016) Pre-earthquake and post-earthquake retrofitting of poorly detailed exterior RC Beam-to-column joints. Eng Struct 109:1–15. https://doi.org/10.1016/j.engstruct.2015.11.009
Kanchanadevi A, Ramanjaneyulu K (2021) Non-invasive hybrid retrofit for seismic damage mitigation of gravity load designed Exterior Beam–Column Sub-assemblage. J Earthq Eng 25(8):1590–1615. https://doi.org/10.1080/13632469.2019.1592790
Khan MI, Al-Osta MA, Ahmad S, Rahman MK (2018) Seismic behavior of beam-column joints strengthened with ultra-high performance fiber reinforced concrete, Compos. Struct., vol. 200, no. May, pp. 103–119, https://doi.org/10.1016/j.compstruct.2018.05.080

Khan SA, Pilakoutas K, Hajirasouliha I, Garcia R, Guadagnini M (2018b) Seismic risk assessment for developing countries: Pakistan as a case study. Earthq Eng Eng Vib 17(4):787–804. https://doi.org/10.1007/s11803-018-0476-3

Kolozvari K, Abdullah S, Wallace J, Kajiwara K (2023) Assessment of the 2015 full-scale ten-story RC test structure using ASCE/SEI 41. Bull Earthq Eng no 012345678910.1007/s10518-023-01657-3

Li B, Kai Q, Xue W (2012) Effects of eccentricity on the Seismic Rehabilitation performance of Non-seismically detailed interior beamwide column joints. J Compos Constr 16(5):507–519. https://doi.org/10.1061/(asce)cc.1943-5614.0000287

Ma CK, Awang AZ, Omar W, Pilakoutas K, Tahir MM, Garcia R (2015) Elastic design of slender high-strength RC circular columns confined with external tensioned steel straps. Adv Struct Eng 18(9):1487–1499. https://doi.org/10.1260/1369-4332.18.9.14

Ma CK, Awang AZ, Garcia R, Omar W, Pilakoutas K, Azimi M (2016) Nominal curvature design of circular HSC columns confined with post-tensioned steel straps. Struct 7:25–32. https://doi.org/10.1016/j.istruc.2016.04.002

Ma CK, Awang AZ, Omar W, Liang M, Jaw SW, Azimi M (2016a) Flexural capacity enhancement of rectangular high-strength concrete columns confined with post-tensioned steel straps: experimental investigation and analytical modelling. Struct Concr 17(4):668–676. https://doi.org/10.1002/suco.201500123

Ma CK, Garcia R, Yung SCS, Awang AZ, Omar W, Pilakoutas K (2019) Strengthening of pre-damaged concrete cylinders using post-tensioned steel straps, Proc. Inst. Civ. Eng. Struct. Build., vol. 172, no. 10, pp. 703–711, https://doi.org/10.1680/jstbu.18.00031

Moghaddam H, Samadi M, Pilakoutas K, Mohebbi S (2010) Axial compressive behavior of concrete actively confined by metal strips; part A: experimental study. Mater Struct 43(10):1369–1381. https://doi.org/10.1617/s11527-010-9588-6

Mostofinejad D, Akhlaghi A (2017) Experimental investigation of the efficacy of EBROG Method in Seismic Rehabilitation of Deficient Reinforced concrete Beam–Column joints using CFRP sheets. J Compos Constr 21(4):1–15. https://doi.org/10.1061/(asce)cc.1943-5614.0000781

Mostofinejad D, Hajrasouliha M (2019) 3D beam–column corner joints retrofitted with X-shaped FRP sheets attached via the EBROG technique, Eng. Struct., vol. 183, no. January, pp. 987–998, https://doi.org/10.1016/j.engstruct.2019.01.038

Muthupriya P, Boobalan SC, Vishnuram BG (2014) Behaviour of fibre-reinforced high-performance concrete in exterior beam-column joint. Int J Adv Struct Eng 6(3). https://doi.org/10.1007/s40091-014-0057-2

Obaidat YT, Abu-Farsakh GAFR, Ashteyat AM (2019) Retrofitting of partially damaged reinforced concrete beam-column joints using various plate-configurations of CFRP under cyclic loading. Constr Build Mater 198:313–322. https://doi.org/10.1016/j.conbuildmat.2018.11.267

Park S, Mosalam KM (2012) Parameters for shear strength prediction of exterior beam-column joints without transverse reinforcement. Eng Struct 36:198–209. https://doi.org/10.1016/j.engstruct.2011.11.017

Park S, Mosalam KM (2013) Experimental investigation of Nonductile RC Corner Beam-Column joints with floor slabs. J Struct Eng 139(1):1–14. https://doi.org/10.1061/(asce)st.1943-541x.0000591

Rajagopal S, Prabavathy S (2015) Investigation on the seismic behavior of exterior beam–column joint using T-type mechanical anchorage with hair-clip bar. J King Saud Univ - Eng Sci 27(2):142–152. https://doi.org/10.1016/j.jksues.2013.09.002

Sasmal S et al (2011) Seismic retrofitting of nonductile beam-column sub-assemblage using FRP wrapping and steel plate jacketing. Constr Build Mater 25(1):175–182. https://doi.org/10.1016/j.conbuildmat.2010.06.041

Setkit M, Imjai T (2019) Strengthening performance of damaged concrete beams in Service conditions using Post-tensioned Metal Strapping technique. J King Mongkut's Univ Technol North Bangkok 29(4):577–584. https://doi.org/10.14416/j.kmutnb.2019.09.004

Setkit M, Imjai T, Chaisakulkiet U, Garcia R, Dangyem RK, Sanupong K, Chamnankit W (2020) Torsional strengthening of low-strength RC beams with post-tensioned metal straps: an experimental investigation. Walailak J Sci Technol 17(12):1399–1411

Sharma R, Bansal PP (2019) Behavior of RC exterior beam column joint retrofitted using UHP-HFRC. Constr Build Mater 195:376–389. https://doi.org/10.1016/j.conbuildmat.2018.11.052

Sharma A, Eligehausen R, Reddy GR (2011) A new model to simulate joint shear behavior of poorly detailed beam-column connections in RC structures under seismic loads, part I: Exterior joints. Eng Struct 33(3):1034–1051. https://doi.org/10.1016/j.engstruct.2010.12.026

Sianko I et al (2020) A practical probabilistic earthquake hazard analysis tool: case study Marmara region. Bull Earthq Eng 18(6). https://doi.org/10.1007/s10518-020-00793-4

Singh V, Bansal PP, Kumar M, Kaushik SK (2014) Experimental studies on strength and ductility of CFRP jacketed reinforced concrete beam-column joints. Constr Build Mater 55:194–201. https://doi.org/10.1016/j.conbuildmat.2014.01.047

Torabi A, Maheri MR (2017) Seismic repair and retrofit of RC Beam-column joints using stiffened steel plates. Iran J Sci Technol - Trans Civ Eng 41(1):13–26. https://doi.org/10.1007/s40996-016-0027-y

Truong GT, Dinh NH, Kim JC, Choi KK (2017) Seismic performance of Exterior RC Beam–column joints retrofitted using various Retrofit solutions. Int J Concr Struct Mater 11(3):415–433. https://doi.org/10.1007/s40069-017-0203-x

Wang GL, Dai JG, Bai YL (2019) Seismic retrofit of exterior RC Beam-column joints with bonded CFRP reinforcement: an experimental study. Compos Struct 224:111018. https://doi.org/10.1016/j.compstruct.2019.111018

Yang Y, Feng S, Xue Y, Yu Y, Wang H, Chen Y (2019) Experimental study on shear behavior of fire-damaged reinforced concrete T-beams retrofitted with prestressed steel straps. Constr Build Mater 209:644–654. https://doi.org/10.1016/j.conbuildmat.2019.03.054

Zabihi A, Tsang HH, Gad EF, Wilson JL (2018) Seismic retrofit of exterior RC beam-column joint using diagonal haunch, Eng. Struct., vol. 174, no. July, pp. 753–767, https://doi.org/10.1016/j.engstruct.2018.07.100

Zamani Beydokhti E, Shariatmadar H (2016) Strengthening and rehabilitation of exterior RC beam–column joints using carbon-FRP jacketing. Mater Struct 49(12):5067–5083. https://doi.org/10.1617/s11527-016-0844-2

Authors and Affiliations

Yasser Helal[1] · Reyes Garcia[2] · Thanongsak Imjai[3] · Pakjira Aosai[3] · Maurizio Guadagnini[4] · Kypros Pilakoutas[4]

✉ Reyes Garcia
reyes.garcia@warwick.ac.uk

[1] AECOM Ltd, Manchester, UK

[2] Civil Engineering Stream, School of Engineering, The University of Warwick, CV4 7AL Coventry, UK

[3] School of Engineering and Technology, Center of Excellence in Sustainable Disaster Management, Walailak University, 80161 Nakhonsithammarat, Thailand

[4] Department of Civil and Structural Engineering, The University of Sheffield, Sheffield S1 3JD, UK